Submitted to Physical Review C

LBL-2680
Preprint c.2

^{7}Be PRODUCTION CROSS SECTIONS IN ^{14}N, ^{12}C, ^{11}B, AND ^{10}B WITH 740-MeV PROTONS

Jonathan R. Radin, Elie Gradsztajn, and Alan R. Smith

March, 1974

Prepared for the U. S. Atomic Energy Commission
under Contract W-7405-ENG-48

RECEIVED
LAWRENCE
RADIATION LABORATORY

FEB 28 1975

LIBRARY AND
DOCUMENTS SECTION

LAWRENCE BERKELEY LABORATORY
UNIVERSITY OF CALIFORNIA
BERKELEY
3Hc

TWO-WEEK LOAN COPY

This is a Library Circulating Copy which may be borrowed for two weeks. For a personal retention copy, call Tech. Info. Division, Ext. 5545

LBL-2680 c.2

DISCLAIMER

This document was prepared as an account of work sponsored by the United States Government. While this document is believed to contain correct information, neither the United States Government nor any agency thereof, nor the Regents of the University of California, nor any of their employees, makes any warranty, express or implied, or assumes any legal responsibility for the accuracy, completeness, or usefulness of any information, apparatus, product, or process disclosed, or represents that its use would not infringe privately owned rights. Reference herein to any specific commercial product, process, or service by its trade name, trademark, manufacturer, or otherwise, does not necessarily constitute or imply its endorsement, recommendation, or favoring by the United States Government or any agency thereof, or the Regents of the University of California. The views and opinions of authors expressed herein do not necessarily state or reflect those of the United States Government or any agency thereof or the Regents of the University of California.

^{7}Be PRODUCTION CROSS SECTIONS IN ^{14}N, ^{12}C, ^{11}B, AND ^{10}B WITH 740-MeV PROTONS*

Jonathan R. Radin† and Elie Gradsztajn
Tel Aviv University, Department of Physics and Astronomy
Ramat-Aviv, Israel

and

Alan R. Smith
Lawrence Berkeley Laboratory, University of California
Berkeley, California 94720

ABSTRACT

A fundamental problem in cosmic ray physics is the production and propagation of Be. We have measured the cross section at 740 MeV for ^{7}Be production in ^{14}N (10.9 mb ± 6%), ^{12}C (9.82 mb ± 6%), ^{11}B (4.17 mb ± 7%), and ^{10}B (6.31 mb ± 7%). The monitor reactions were ^{12}C (p, pn) ^{11}C = 29.9mb ± 5% and the ^{12}C(p, x) ^{7}Be cross section listed above.

I. INTRODUCTION

The source of L nuclei (Li, Be, B) in cosmic rays is, by concensus,[1] the spallation of heavier nuclei -- primarily M nuclei (C, N, O) -- in interaction with the interstellar gas (≈ 90% H and 10% He).[2] The production of the three Be isotopes (atomic numbers 7, 9, and 10) are of great interest[3,4] because ^{10}Be with a half-life of 1.5 Myr[5] may serve as a cosmic ray dating tool. An important ^{10}Be production mechanism is the ^{11}B(p, 2p)^{10}Be reaction, which cross section was measured by Raisbeck and Yiou[6,5] at 150 and 600 MeV. Their monitor reaction was ^{11}B(p, x)^{7}Be, which they separately measured relative to the ^{27}Al(p, x) ^{22}Na monitor reaction. Since they record accuracies of ± 20% for the last measurement, we have repeated the ^{10}B(p, x)^{7}Be and ^{11}B(p, x)^{7}Be measurements relative to the ^{12}C(p, pn)^{11}C and ^{12}C(p, x)^{7}Be monitor reactions. We have also measured the ^{14}N(p, x)^{7}Be cross section relative to the same two monitor reactions, as there is a dearth of accurate measurements for this important cosmic-ray spallation reaction. We measured the ^{12}C(p, x)^{7}Be cross section relative to the ^{12}C(p, pn)^{11}C monitor reaction and used our new value for this monitor reaction when calculating the cross sections.

II. EXPERIMENTAL TECHNIQUES

Sandwiches 3.81 cm in diameter, consisting of a target powder compressed into a self-supporting disk, and a beam monitor, were exposed in the 740-MeV external proton beam of the 184-in. cyclotron at Lawrence Berkeley Laboratory (LBL); see Fig. 1. The target powders

were: natural boron[7] (80.4% ^{11}B and 19.6% ^{10}B with ≈0.6% impurity, 0.57 g cm^{-2} thick); boron enriched with ^{10}B[8] (92.01% ^{10}B and 7.99% ^{11}B with ≈ 5% impurity, 0.44 g cm^{-2} thick); boron nitride[9] (99% BN with ≈ 1% impurity, 0.60 g cm^{-2} thick). The beam monitors were polystyrene disks 2 mm thick (0.21 g cm^{-2}). The beam monitor cross sections were $^{12}C(p,pn)^{11}C$ with a value of 29.9 mb ± 5%;[10] and for the B, $^{10}B_{enriched}$ and BN targets we also used the $^{12}C(p,x)^{7}Be$ cross section with a value of 9.82 mb ± 6% which we measured and report in this paper. The decay parameters[11,12] used were: for ^{7}Be a 53.3-day half-life with a 0.103 branching ratio to the 478-keV level of ^{7}Li; for ^{11}C a 20.35-min half-life. Three exposures, each with new constituents, were made for each of the three target substances. These nine exposures of the target-powder monitor-disk sandwiches were also used to measure the $^{12}C(p,x)^{7}Be/^{12}C(p,x)^{11}C$ ratio (and the subsequent cross section) in the nine polystyrene monitor disks of the sandwiches. The exposures were for ≈ 3 min. A He-filled ionization chamber situated ≈ 20 cm downstream of the targets was used to monitor the constancy of the beam flux. The digitalized ionization chamber current was recorded every 30 sec. The beam-flux fluctuations, rms-averaged over the exposure time, were less than 5%. After irradiation the target powders were placed in Cu jackets and sealed.

All targets were counted on a 20.3-cm-diam × 10.2-cm-thick NaI(Tl) crystal detector and/or on a 10 cm^3 planar Ge(Li) detector (resolution: FWHM = 2.2 keV at 480 keV) located in the concrete-shielded low-background cave of the Health Physics group at LBL.[13]

The multichannel analyzer of the two detector systems is a Victoreen SCIPP 1600-channel analyzer, which when operated with the NaI detector included a digital gain stabilizer. For ^{7}Be decay counting on the NaI detector the gain was stabilized on the 478-keV peak, and for β^+ decay counting on the 511-keV peak. The peak interval for analysis was 380-610 keV for both decays.

A. The $^{12}C(p,x)^{7}Be$ Cross Section

About 180 min after each exposure the polystyrene targets were placed between Cu plates (serving as β^+ annihilators) and were counted on the NaI system. The analysis of the counting-system dead time, detailed in a previous report,[14] was improved so that β^+ decaying targets could be counted to count rates of 1M min^{-1} with less than 0.2% deviation in the fitted initial activity (see Appendix). Initial count rates on the NaI detector were < 750 K min^{-1}. The ^{11}C decay was counted at 2-min intervals for at least 2-3 half-lives. The ^{11}C decay was fitted to a single-component exponential decay (20.35-min half-life) with a constant background (equal to the ^{7}Be activity, which was determined later, plus the target-absent environmental activity of the detector which was constant to 2%). The background was also set as a free parameter and the resultant fitted ^{11}C activity agreed to ±0.3% with the fixed background fitting. The χ^2/n (n = degree of freedom) of the nine decay fits were 0.4–3. The uncertainty in the fitted ^{11}C activity was taken as $[(\chi^2/n)\, d_{1,1}^2]^{1/2}$, where $d_{1,1}$ is the diagonal element of the inverse error matrix (one-dimensional in this case). During the 90 days following the exposures, the polystyrene targets were counted

between the Cu plates on the NaI system 2-4 times for ^{7}Be decay. The ^{7}Be decay was fitted to a single-component exponential decay (53.3-day half-life) with a constant background (measured with no target in place). The uncertainty in the fitted ^{7}Be activity was determined from the same formula used for the ^{11}C uncertainty. The χ^2/n of the ^{7}Be decay fits were 0.2-7 except for two runs with χ^2/n of 640 and 35. No source of error was found as a cause of these two poor fits. The values of the $^{12}C(p,x)^{7}Be/^{12}C(p,pn)^{11}C$ ratio, corrected for the secondary effects discussed below but with only the errors from the fits (described above, and then rms-combined), are tabulated in TableII. The cross-section ratios associated with the two large χ^2/n values of 640 and 35 are runs No. 5 and 6 (Table II), which differ from the mean cross-section ratio by 6% and 0.5% respectively. The cross-section ratios were weighted by the fit uncertainty (Table II) in forming the mean cross section ratio. Thus the fit with $\chi^2/n = 640$, which has a relatively large error of 4% (Table II, run No. 5) makes a small contribution to the mean.

The $^{12}C(p,x)^{7}Be/^{12}C(p,pn)^{11}C$ ratio was corrected for the following experimentally determined effects (Table I, last section): i) the differences in absorption efficiency (for removal from the NaI photopeak) between the 478-keV (^{7}Be) and 511-keV (^{11}C) γ rays in their traversal of the stainless steel housing of the NaI $(1.5 \pm 0.4)\%$, and in their traversal of the Cu-plate target holders $(1.9 \pm 0.3)\%$ [which when combined with a $(-2.4 \pm 1)\%$ [15] difference in the NaI photoabsorption efficiency for these two γ rays yielded a correction of $(1 \pm 1)\%$]; ii) the coincidence sum peak of the two annihilation γ's of the β^+ decay $(-5.7 \pm 0.2)\%$.[16] The weighted mean of the $^{12}C(p,x)^{7}Be/^{12}C(p,pn)^{11}C$ ratio corrected for secondary

effects is 0.3285, with an uncertainty of 0.5% from the decay fits and 2% from the secondary effects, which rms-combine to an error of 2% (Table II). The $^{12}C(p,x)^{7}Be$ cross section, based on a $^{12}C(p,pn)^{11}C$ cross section of 29.9 mb± 5%,[10] is 9.82 mb± 6% (Table III).

B. The $B(p,x)^{7}Be$ and $^{10}B(p,x)^{7}Be$ Cross Section

About 90 days after exposure the B and $^{10}B_{enriched}$ targets, and their associated polystyrene monitor disks, were counted on the Ge detector (the β^{+} contamination of the B and $^{10}B_{enriched}$ targets was never small enough to allow counting on the NaI crystal). The linear thickness of the polystyrene disks was one-half the linear thickness of the B and ^{10}B target. The polystyrene disks were counted with a dummy polystyrene disk in a Cu jacket identical to those housing the target powders. A correction of (10.7± 2)%, (see section E, and Table 1, row 4) compensated for the different counting configurations of the targets and monitors.

C. Peak and Decay Fitting

The ^{7}Be (478-keV) peak counts on the Ge system were analyzed with the computer program SAMPO.[17] In this program the peak shape is characterized by three parameters relating to i) the width of the central Gaussian, and ii) the two junction points between the central Gaussian and the upper and lower tailing exponentials. These three parameters, for each target counting, were varied by allowing SAMPO to find the best parameters, and by then supplying slightly different parameters. In addition, using the parameters determined by SAMPO,

we varied the width and center of the fitting interval for the ^{7}Be peak. For each alteration in the fitting, we tabulated: i) the ^{7}Be peak counts, ii) the percent fit error [(pfe) = $(\chi^2/n)^{1/2} d_{i,i}$, where $d_{i,i}$ is the diagonal element of the inverse error matrix associated with the peak height], and iii) the visual quality of the peak and continuum shapes [quantities (i) and (ii) are listed in the SAMPO output]. The largest deviations in the ^{7}Be peak counts amongst the various fittings were less than 6% (the worst fittings had poor peak and continuum shapes, and large pfe). The fit with the best peak and contiuum shapes was almost invariably the fit with the lowest pfe. In cases when two different fits were associated with these two measures of the goodness-of-fit, the difference in the ^{7}Be peak area counts between the two fits was < 0.3%. We used the criteria of best peak and continuum shape to choose the fitted ^{7}Be peak counts. The peak fitting algorithm of SAMPO employs the routine VARMIT,[18] whose path of minimalization approaches the data from below, and thus the best fit always underestimates the data. This is a small effect here {≡ ve ≈ [(sum data points) - (sum fitted points)]/(sum data points) < 1.2%} and is partially canceled when we form the ratio of target/monitor activity. We include this anomaly in the uncertainty associated with each fit, which was taken as $(\mathrm{pfe}^2 + \mathrm{ve}^2)^{1/2}$ and was <2.3% for all of the Ge-counted targets and monitors (Table I, row 1). We formed the B(p, x) ^{7}Be/^{12}C(p, x) ^{7}Be and ^{10}B$_{\mathrm{enriched}}$ (p, n) ^{7}Be/ ^{12}C(p, x) ^{7}Be ratios from their respective monitors, all counted on the Ge detector. To use the ^{12}C(p, pn) ^{11}C monitor we factored the cross-section ratios; e.g., for a boron target we have

$$\frac{\mathrm{B(p,x)}\,^7\mathrm{Be}}{^{12}\mathrm{C(p,pn)}\,^{11}\mathrm{C}} = \left[\frac{\mathrm{B(p,x)}\,^7\mathrm{Be}}{^{12}\mathrm{C(p,x)}\,^7\mathrm{Be}}\right]_{\mathrm{Ge}} \left[\frac{^{12}\mathrm{C(p,x)}\,^7\mathrm{Be}}{^{12}\mathrm{C(p,pn)}\,^{11}\mathrm{C}}\right]_{\mathrm{NaI}},$$

where the subscripts refer to the detector on which the targets inside the brackets were counted. The second bracket was formed for each target powder from the same polystyrene monitor disk that was used to form the first bracket, and in fact was previously determined for the $^{12}C(p, x)^{7}Be$ measurement. In this manner, by counting and/or analyzing on the Ge detector only the ^{7}Be decay components, we remove two potentially large sources of systematic error in using Ge detectors: i) the big difference in Ge photopeak efficiency between 478-keV (^{7}Be) and 511-keV (^{11}C) γ rays of $\approx 11\%$; and ii) the use of calibrating sources whose distribution of activity, and thus solid angle exposed to the relatively small Ge-detector area, differs from that of the irradiated targets and monitors which were exposed in a broad beam (the targets and monitors of course have the same distribution of activity). These systematic effects are transferred to the large NaI detector whose large volume and high Z result in its photopeak efficiency being much less sensitive than is the photopeak efficiency of Ge, to the energy and spatial distribution of the incoming γ irradiation. The difference in efficiency of the 20.3-cm-thick $\times$ 10.2-cm-thick NaI crystal between the 478-keV and 511-keV γ energy was taken from Green and Finn[15] as $(2.4 \pm 1)\%$. Additional corrections to the B and $^{10}B_{enriched}$/monitor cross section ratios are described in section E and Table I.

D. BN Targets

About 90 days after exposure the BN targets and their associated polystyrene monitors were counted on the NaI detector 2-4 times

for ^{7}Be activity (after prior verification on the Ge detector that the 511-/478-keV peak ratios were < 0.5%). The secondary corrections to the BN(p, x)^{7}Be/^{12}C(p, x)^{7}Be ratio are discussed below and are tabulated in Table I. The BN(p, x)^{7}Be/^{12}C(p, x)^{11}C ratio was factorized and developed in the same manner as was the B(p, x)^{7}Be/^{12}C(p, pn)^{11}C ratio except that all targets and monitors were counted on the NaI detector. The ^{14}N(p, x)^{7}Be/^{12}C(p, x)^{7}Be and ^{14}N(p, x)^{7}Be/^{12}C(p, pn)^{11}C ratios were formed by subtracting the B/monitor ratios from the corresponding BN/monitor ratios.

E. Calibrations and Secondary Effects

The increase in ^{7}Be production as a function of target thickness traversed by the proton beam (depth effect) was estimated by exposing a three-piece target sandwich 3.81 cm in diam consisting of thin (2.15 g cm^{-2}) - thick (17.9 g cm^{-2})- thin (2.15 g cm^{-2}) disks of BN (95% BN), with 0.008 g cm^{-2} polyethylene front and rear pieces which provided ^{7}Be forward and backward equilibrium production for the front and rear BN pieces. The front and rear thin BN pieces were counted on the NaI system and yielded a percent increase in ^{7}Be production of (1.0± 0.2)% per mean g cm^{-2} BN in front of the target. This depth correction was applied to all targets and products and was < 0.5% in all cases. The analysis of the absorption difference between the 478-and 511-keV γ rays in the NaI crystal and its housing, and in the Cu target and monitor holders, is found in section A.

The compressed target powders had twice the linear thickness of the polystyrene monitor. The polystyrene monitor disks were counted on the Ge detector with a dummy nonactive disk, in order to have the same linear target thickness during decay counting. We estimated this target-thickness effect by reversing the position of the polystyrene monitor and dummy inside the target holder and then averaging the results (Table I, row 4) of the two counting configurations. A 1% systematic error was included in the Ge detector measurements with this target-thickness correction. All target holders were intercalibrated with ^{7}Be, $^{64}Cu(\beta^{+})$, and/or ^{137}Cs(663 keV) sources (Table I).

The combined C+N contamination in the B target was analyzed (by Pregle combustion and Durnas methods)[19] to be (1.3±1)%. We estimated the O contamination as (1 ±1)% and the combined CNO contamination as 2.3%, which, with an average ^{7}Be production cross section of 10 mb, resulted in a (1.7±1.7)% lowering of the $B(p,x)^{7}Be/^{12}C(p,x)^{7}Be$ ratio. The effect of the heavy-element contamination (±1%) on this cross section/monitor ratio was estimated as ±1%. The composition of the $^{10}B_{enriched}$ target was taken from the vendor's[8] analysis which was 4.89% contaminant consisting of 3.6% O, 0.98% C, and 1.8% of heavier material primarily Cu, Al, K, and Si. The heavier elements have small ^{7}Be production cross sections at 740 MeV and on a per-nucleon basis their effective ^{7}Be production is 0.1-0.3 that of B. To compensate for heavy elements present in the $^{10}B_{enriched}$ target we reduced the weight of the $^{10}B_{enriched}$ target (for the cross section calculation) by (1±1)%.

The effect of the 0 and C contamination of the $^{10}B_{enriched}$ target was estimated from their measured ^{7}Be production cross sections of 8.2± 1 mb[20,21] and 10.9± 1 mb[10] respectively at 740 MeV and resulted in a (0.7± 0.7)% reduction in the $^{10}B_{enriched}(p,x)^{7}Be/^{12}C(p,x)^{7}Be$ ratio. The BN target contamination was taken as ± 1%; little contaminating radiation was present. In Table I is tabulated the secondary corrections and uncertainties. Table I is delineated into those corrections which were made to the individual target/monitor ratios, and to those made to the mean target/monitor ratios.

III. RESULTS AND CONCLUSIONS

The target/monitor ratios and the resultant cross sections are tabulated in Table III. The final cross-section values are the average of the two monitor results. As the errors are dependent, the final error is the average error of the two monitor results. In Table IV we compare our results with previous measurements and compilations from the literature.[20,22-27] Our $^{12}C(p,x)^{7}Be$ cross section is (11± 12) % less than the value in the Cumming compilation.[10] His excitation function at this energy is based on measurements made relative to the $^{27}Al(p,x)^{24}Na$ monitor reaction. This reaction is sensitive to contaminating low-energy (evaporation) neutrons via the $^{27}Al(n,\alpha)^{24}Na$ reaction.[28] We suspect that this monitor reaction is at fault. The $^{14}N(p,x)^{7}Be$ cross section (Table IV and Fig. 2) appears constant in the energy range 730 MeV-5.7 GeV (within experimental errors) with a value of 11± 1 mb. The same result is observed for the $^{12}C(p,x)^{7}Be$ cross section.[10] The $^{16}O(p,x)^{7}Be$ excitation function

compiled by Audouze, Epherre, and Reeves[22] shows a rise in this energy region but the data are sparse. A constant nuclear cross section defines the asymptotic region and is a requirement for factorization, currently being investigated by Heckman et al., at 2.1 GeV/N.[29]

Our $^{11}B(p,x)^{7}Be$ cross section is the same as that measured by Raisbeck and Yiou[6] at 600 MeV but with improved accuracy. If the $^{11}B(p,2p)^{10}Be/^{11}B(p,x)^{7}Be$ ratio is constant between 600 and 740 MeV, then the uncertainty in the $^{11}B(p,2p)^{10}Be$ cross section is reduced to $\approx$ 30%, and the cross section has the value 14 ± 4 mb[6,5] at 740 MeV.

IV. APPENDIX

Dead time of the NaI detector system. A polystyrene disk, with initial ^{11}C activity in the β^{+} photopeak on the NaI system of 5 M counts min^{-1} was counted at 2-min intervals until the count rate was 30 K min^{-1}. The computer fitting routine for calculating initial ^{11}C activity contained a deadtime correction of the form exp (CR$\times\tau$), where CR is the count rate and τ is the dead time. For different initial count rates at the commencement of the fitting routine, we varied τ and observed the χ^2 of the decay fit. The best value for τ (minimum χ^2) increased by 10% between initial count rates of 250 k min^{-1} to 1 M counts min^{-1}, with a resulting ^{11}C variation of 0.2%.

ACKNOWLEDGMENTS

This work commenced with the suggestion to measure the $^{11}B(p,x)^{7}Be$ cross section, made to the authors several years ago by René Bernas (since deceased). We thank Al Stetz for the use of his ionization chamber and associated equipment, and we thank Steven Kruger for aid in fabricating the targets.

Footnotes and References

*Work done under the auspices of the U.S. Atomic Energy Commission.

†Present address: Laboratoire Rene Bernas, Batiment 108, B.P.I., 91406- Campus-Orsay, France.

[1]M. M. Shapiro and R. Silberberg, Ann. Rev. Nucl. Sci. 20 (1970).

[2]I. J. Danziger, Ann. Rev. Astron. Astrophys. 8 (1970).

[3]F. W. O'Dell, M. M. Shapiro, R. Silberberg, and C. H. Tsao, New Observations of Be/B in Cosmic Rays, in Proc. 13th International Cosmic Ray Conf., paper 146, Denver, Colorado, 1973 (unpublished).

[4]G. Raisbeck and F Yiou, The ^{10}Be Problem-Myth vs Reality, Proc. 13th International Cosmic Ray Conf., paper 253, Denver, Colorado, 1973 (unpublished).

[5]F Yiou and G. Raisbeck, Phys. Rev. Lett 29, 372 (1972).

[6]G. M. Raisbeck and F. Yiou, Phys. Rev. Lett. 27, 875 (1971).

[7]Ventron Corp., Alfa Products, P. O. Box 159, Beverly, Mass. 01915.

[8]Oak Ridge National Laboratory, Isotope Sales Div., P. O. Box X, Oak Ridge, Tenn. 37830.

[9]Fluka AG, Chemische Fabrik, CH-9470 Buchs SG, Switzerland.

[10]J. B. Cumming, Ann. Rev. Nucl Sci 13 (1963).

[11]C. M. Lederer, J. M. Hollander, and I. Perlman, Table of Isotopes, 6th ed. (Wiley, New York, 1967).

[12]Nuclear Data Tables 8, 146 (1970).

[13] W. S Gilbert, D. Keefe, J. B. McCaslin, H. W. Patterson, A.R. Smith, L. D. Stephens, K. B. Shaw, G. R. Stevenson, R. H. Thomas, R. D. Fortune, and K. Goebel, Lawrence Radiation Laboratory Report UCRL-17941, 1968 (unpublished).

[14] J. R. Radin, Ph.D thesis, New York University, 1971 (unpublished).

[15] R. M. Green and R. J. Finn, Nucl. Instrum. Methods 34, 72 (1965).

[16] J R. Radin, A. R. Smith, and N. Little, Phys. Rev. C 9, 1718 (1974).

[17] J. T Routti and S. G. Prussin, Nucl. Instrum. Methods 72, 125 (1969); J. T. Routti, Lawrence Radiation Laboratory Report UCRL-19452, 1969 (unpublished).

[18] W. C. Davidson, Variable Metric Method for Minimalization, ANL-5990 (1959); E. Beals, VARMIT, Lawrence Radiation Laboratory Memo BK Y-ZO (unpublished).

[19] Performed by V. Tashinian, University of California, College of Chemistry, Berkeley, Ca 94720.

[20] P. L. Reeder, J. Inorg. Nucl. Chem. 27, 1879 (1965).

[21] R. Silberberg and C H. Tsao, Astrophys. J. Suppl. Ser.No.220, 25, 315 (1973).

[22] J. Andouze, M. Epherre, and H Reeves, in High Energy Nuclear Interactions in Astrophysics, edited by B.S P. Shen (Benjamin, New York, 1967).

[23] R. George, These Zerne cycle, Institute de Physique Nucleaire, Orsay, 1962 (unpublished), as quoted in Ref. 22.

[24] L. Valentin, G. Albouy, J. P. Cohen, and M. Gusakow, Phys. Lett. 7, 163 (1963).

[25] P. A. Benioff, Phys. Rev. 119, 316 (1960), as quoted in Ref. 22.

[26] M. Barbier and S. Regnier, J. Inorg. Nucl. Chem. 33, 2720 (1971).

[27] M. Honda and D. Lal, Phys. Rev. 118, 1618 (1960).

[28] A. F. Stehney and E. P. Steinberg, Nucl. Instrum. Methods 59, 102 (1968).

[29] H. H Heckman, D. E Greiner, P. J. Lindstrom, and F. S. Bieser, Phys. Rev. Lett. 28, 926 (1972).

Table I. Secondary effects, corrections and uncertainties for the target/monitor cross-section ratios (Table II).

Corrections to the individual target/monitor ratios of Table II

Effect	Correction to targets (percent ± percent) B and $^{10}B_{enriched}$		BN	
^{7}Be decay fit		±(0.7-2.3)		±< 1
^{7}Be buildup in target from secondaries	< -0.5		< -0.5	
Target holder intercalibration		± 2		± 1
Target/monitor counting efficiency (a)	10.7	± 2	2.8	± 1
Target alignment during irradiation		± 1		± 1
^{7}Be decay absorption in target		± 1		± 1

Corrections to the mean target/monitor ratios of Table II

	B	$^{10}B_{enriched}$	BN
CNO contamination	-0.7±0.7	-1.7±1.7	± 1
heavy element contamination	±1	1±1	0
systematic error from target holder construction and (a) above	±1	±1	0

Corrections to the $^{12}C(p,x)^{7}Be/^{12}C(p,pn)^{11}C$ ratios of Table II

	B and $^{10}B_{enriched}$	BN
rms sum of ^{7}Be- and ^{11}C-fit uncertainties[a]	0.2-4.	0.09-0.3
β^{+} sum peak in the NaI	-5.7±0.2	-5.7±0.2
^{11}C decay during ≈ 3 min irradiation	-5.	-5.
target holder calibration	±1	±1
difference in absorption between β^{+} and ^{7}Be decay radiation in the NaI(-2.4±1)%, the NaI housing (+1.5±0.4)%, and the target holders (+1.9±0.3)% which combine to	1±1	1±1

[a]Correction to the individual target/monitor ratios. The remaining corrections are to the mean.

Table II. Target/monitor ratios. First column includes the secondary corrections and uncertainties from Table I, part 1. The second column includes the secondary corrections from Table I, part 3; but the uncertainties are only the rms combined ^{7}Be and ^{11}C fit uncertainties. The inclusion of all of the uncertainties from Table I, part 3 raises the error of the mean in the second column to 2%.

Run	$\frac{B(p,x)^{7}Be}{^{12}C(p,x)^{7}Be}$ ±%	$\frac{^{12}C(p,x)^{7}Be}{^{12}C(p,pn)^{11}C}$ ±%
1	0.4973 ± 4.0	0.3305 ± 0.19
2	0.4655 ± 2.8	0.3302 ± 0.26
3	0.4690 ± 2.7	0.3280 ± 0.78
	0.4724 ± 2.0[a]	
	$\frac{^{10}B_{enriched}(p,x)^{7}Be}{^{12}C(p,x)^{7}Be}$ ±%	
4	0.5926 ± 2.8	0.3314 ± 0.37
5	0.6403 ± 3.3	0.3080 ± 4.4
6	0.6537 ± 3.0	0.3268 ± 1.1
	0.6288 ± 4.3[b]	
	$\frac{BN(p,x)^{7}Be}{^{12}C(p,x)^{7}Be}$ ±%	
7	1.573 ± 2	0.3288 ± 0.17
8	1.575 ± 2	0.3268 ± 0.30
9	1.586 ± 2	0.3277 ± 0.09
	1.578 ± 2[b]	0.3285 ± 0.5[c]

[a] Weighted mean.

[b] Unweighted mean.

[c] Weighted mean of the nine exposures.

Table III. Ratios of ^{7}Be production/monitor cross sections at 740 MeV, and resulting ^{7}Be production cross sections. All errors are in percent. The monitor cross sections are $^{12}C(p, pn)^{11}C$ = 29.9 mb ± 5% (from reference 10) and $^{12}C(p, x)^{7}Be$ = 9.82 mb ± 6% (from this work, and based on the above ^{11}C monitor cross section). The $^{10}B_{enriched}$ and BN cross sections are included for convenience.

Target	Ratio to monitor reaction; monitor is		Cross section derived from monitors (mb)		Cross-section average (mb)
	$^{12}C \rightarrow {}^{7}Be$	$^{12}C \rightarrow {}^{11}C$	$^{12}C \rightarrow {}^{7}Be$	$^{12}C \rightarrow {}^{11}C$	
B	0.4645 ± 3.9	0.1530 ± 4.4	4.56 ± 7.2	4.58 ± 6.7	4.57 ± 7
$^{10}B_{enriched}$	0.6309 ± 4.3	0.2030 ± 4.4	6.20 ± 7.4	6.08 ± 6.6	6.13 ± 7
BN	1.578 ± 2	0.5181 ± 2.2	15.5 ± 6.3	15.5 ± 5.5	15.5 ± 6
^{11}B	0.4217 ± 3.7	0.1401 ± 4.5	4.14 ± 7.0	4.19 ± 6.7	4.17 ± 7
^{10}B	0.6491 ± 4.3	0.2085 ± 4.3	6.37 ± 7.4	6.24 ± 6.6	6.31 ± 7
^{14}N	1.114 ± 3.3	0.3651 ± 3.6	10.9 ± 6.9	10.9 ± 6.2	10.9 ± 6
^{12}C	---	0.3285 ± 2	---	9.82 ± 6	9.82 ± 6

Table IV. Cross sections for ^{7}Be production in various targets, from the literature.

E (MeV)	^{14}N σ (mb)	^{12}C σ (mb)	B σ (mb)	^{11}B σ (mb)	^{10}B σ (mb)
150	4.4±1.1[a,b]				
	6.5±1[a,d]			6.9±1.4[c]	8±1.6[c]
225	9.5±0.4[e]				
300	5.8±2[f]		4.5±1.5[f]		
400	10.5±1[e]				
600	7±2[f]		5.5±2[f]	4.2±0.8[c]	5.4±1.1[c]
740	11.4±1[e]				
		10.9±1[g]	4.57±0.3[h]	4.17±0.3[h]	6.31±0.4[h]
	10.9±0.6[h]	9.82±0.6[h]			
2200	8.6±0.8[i]				
5700	12±2[a,j]				

[a]See Ref. 22.

[b]See Ref. 23.

[c]See Ref. 6.

[d]See Ref. 24.

[e]See Ref. 27, and adjusted for ^{7}Be branching ratio of 0.103 and for value of monitor cross section from Ref. 10.

[f]See Ref. 26.

[g]See Ref. 10.

[h]Present work.

[i]See Ref. 20.

[j]See Ref. 25.

FIGURE CAPTIONS

Fig. 1. Target arrangments. Proton beam incident from the left. The open pieces are polystyrene, the hatched pieces are: set (a), B and $^{10}B_{enriched}$; set (b), BN. In set (b) only the first polystyrene piece was counted. Intersticed are 0.008-cm polyethylene sheets.

Fig. 2. The $^{14}N(p,x)^{7}Be$ excitation function from the literature (Table IV). × Refs. 22 and 24; O, Refs. 22 and 23; ●, Ref. 26; △, Ref. 27; ▲, present work; □, Ref. 20; ■, Refs. 22 and 25.

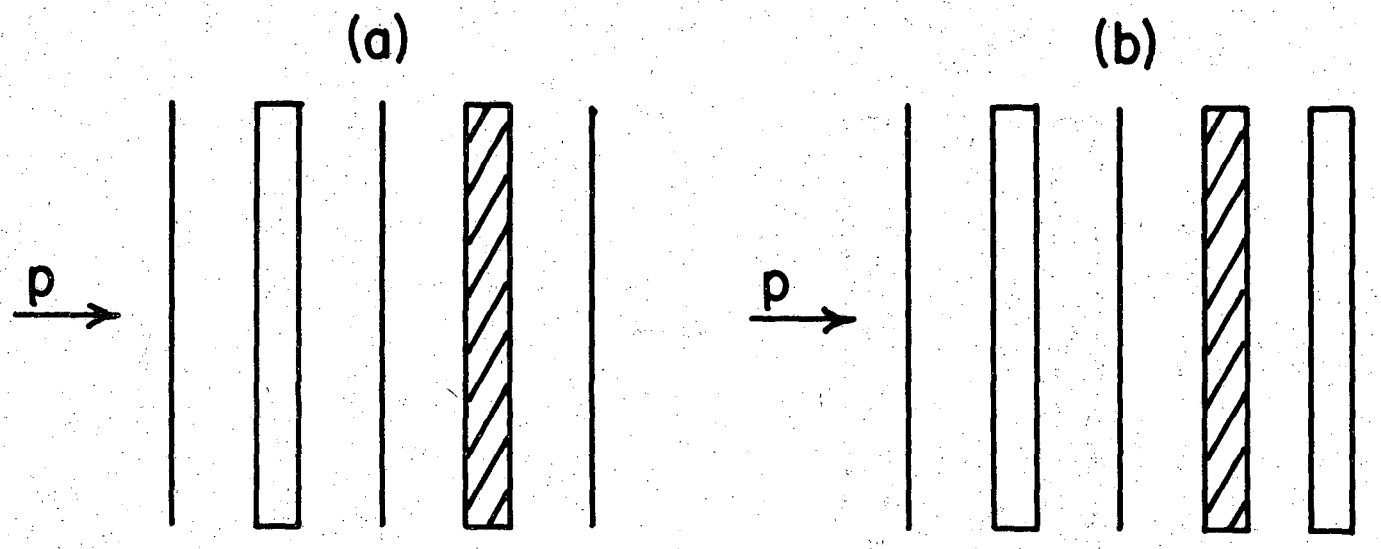

XBL 743-565

Fig. 1

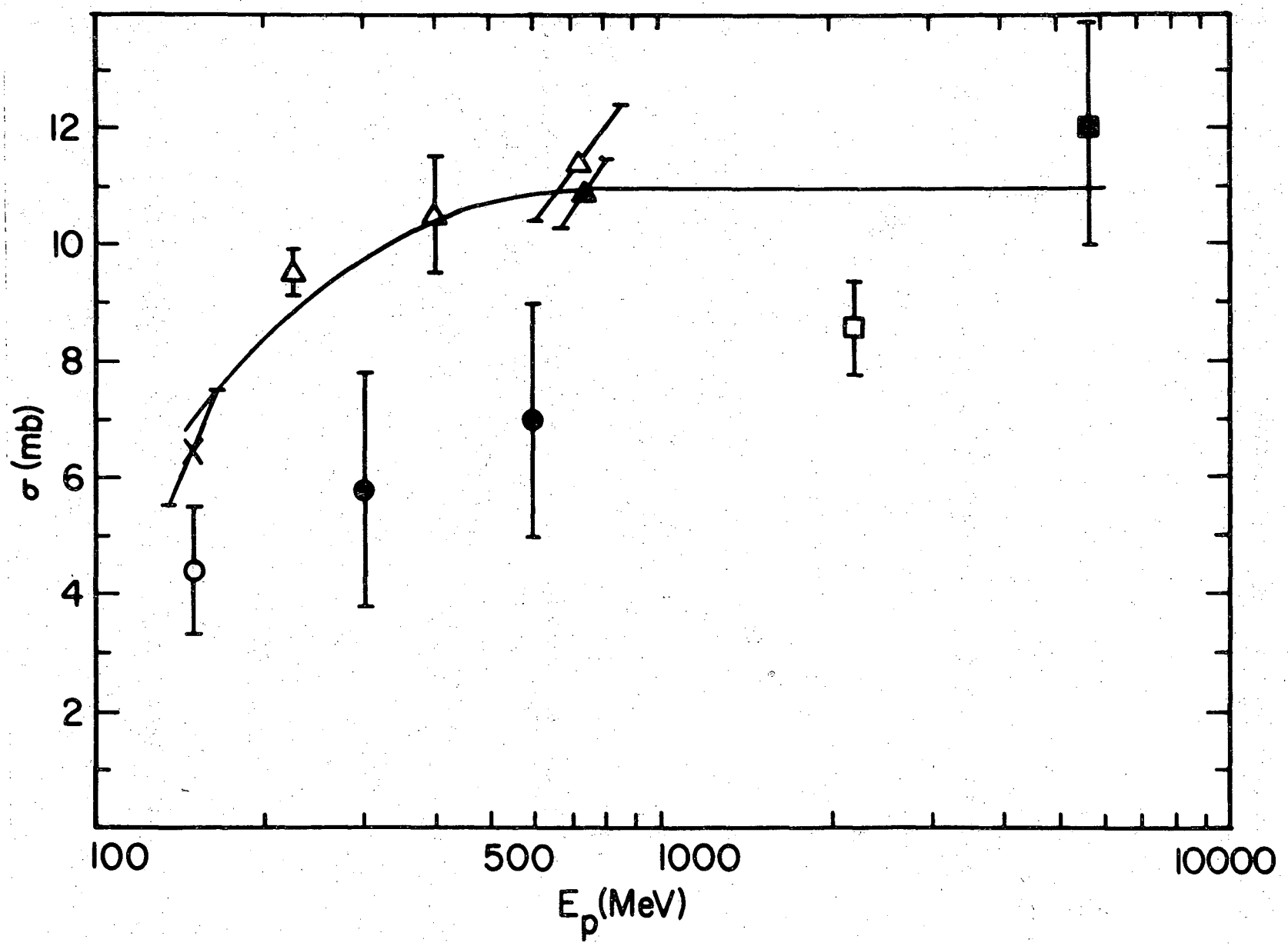

Fig. 2

LEGAL NOTICE

This report was prepared as an account of work sponsored by the United States Government. Neither the United States nor the United States Atomic Energy Commission, nor any of their employees, nor any of their contractors, subcontractors, or their employees, makes any warranty, express or implied, or assumes any legal liability or responsibility for the accuracy, completeness or usefulness of any information, apparatus, product or process disclosed, or represents that its use would not infringe privately owned rights.

TECHNICAL INFORMATION DIVISION
LAWRENCE BERKELEY LABORATORY
UNIVERSITY OF CALIFORNIA
BERKELEY, CALIFORNIA 94720